

LIMITS ON FAILURE SCENARIOS FOR CRAB CAVITIES IN THE HL-LHC *

A. Santamaría García, H. Burkhardt, K. Hernández Chahín, A. Macpherson,
K. Sjobak, D. Wollmann, B. Yee-Rendón, CERN, Geneva, Switzerland

Abstract

The High Luminosity (HL) LHC upgrade aims for a tenfold increase in integrated luminosity compared to the nominal LHC, and for operation at a levelled luminosity of $5 \times 10^{34} \text{ cm}^{-2}\text{s}^{-1}$, which is five times higher than the nominal LHC peak luminosity. Crab Cavities (CCs) are planned to compensate the geometric luminosity loss created by the increased crossing angle by rotating the bunch, allowing quasi head-on collisions at the Interaction Points (IP). The CCs work by creating transverse kicks, and their failure may have short time constants comparable to the reaction time of the Machine Protection System (MPS), producing significant coherent betatron oscillations and fast emittance growth. Simulations of CC failure modes have been carried out with the tracking code SIXTRACK [1], using the newly added functionality called DYNK [2], which allows to dynamically change the attributes of the CCs. We describe these simulations and discuss early, preliminary results.

INTRODUCTION

In order to produce ten times more collisions during the HL-LHC lifetime, the nominal levelled luminosity will be $5 \times 10^{34} \text{ cm}^{-2}\text{s}^{-1}$. An increase in luminosity entails an increase in proton collisions per bunch crossing (pile-up) and a rapid decay of the beam current due to proton burning. In order to optimize the experimental detectors' efficiency, the pile-up has to be maintained at an acceptable level and the luminosity should remain constant over the length of the fill. It has been proposed to maintain the luminosity constant by reducing the transverse beam size by means of reducing β^* , called β^* levelling. A smaller beam size at the IP implies larger beam sizes in the triplet quadrupole magnets, which will need a larger aperture. The implementation of low β^* collision optics will be carried out with the Achromatic Telescopic Squeeze (ATS) scheme [3]. A smaller β^* requires a larger crossing angle θ , which in turn causes a reduction of the geometrical luminosity. The crossing angle will be increased by a factor of two for HL-LHC, causing a significant loss in luminosity and therefore delaying the integrated luminosity goal. CCs have been proposed to counteract this effect. They generate transverse electromagnetic fields, which rotate each bunch longitudinally by $\frac{\theta}{2}$ such that the bunches collide effectively head-on, compensating the geometric luminosity loss. CCs allow access to the full performance reach of the small β^* values offered by the ATS scheme and the larger triplet quadrupole magnets [4, Chapter 1].

* Research supported by the High Luminosity LHC project.

THE MPS AND CRAB CAVITY FAILURES

A variety of processes can cause unavoidable beam losses during normal and abnormal operation. Because of the high stored energy of the HL-LHC beams, above 700 MJ, the beams can be highly destructive. Even a local beam loss of a tiny fraction of the full beam into a superconducting magnet can cause a quench, and large beam losses can cause damage to accelerator components. Because of this, the MPS is designed with very high reliability to prevent an uncontrolled release of the energy and damage due to beam losses [4, Chapter 7].

With the installation of CCs, new failure scenarios that could cause beam losses have to be considered. Voltage or phase changes of the CCs will happen with a time constant τ , which is proportional to the time it takes to dissipate the energy stored in the cavity through the coupler when the RF sources are turned off (external Q factor):

$$\tau = \frac{2 \cdot Q_{\text{ext}}}{\omega},$$

where ω is the angular frequency of the CCs. For the HL-LHC parameters of $f_{\text{cc}} = 400.79 \text{ MHz}$ and $Q_{\text{ext}} = 3 \times 10^5 - 5 \times 10^5$, CC failures could happen with a time constant as fast as $\tau = 238 - 397 \mu\text{s} \approx 2 - 4$ LHC turns. These ultrafast failures are potentially dangerous, which motivates detailed studies as there may not be enough time to extract the beam in a controlled way [5].

SIMULATION SETTINGS

Tracking simulations have been carried out with the collimation version of SIXTRACK and the DYNK module, in order to estimate the beam loss distribution around the ring in case of CC failures. These simulations were carried out for Beam 1 and IP1, considering one bunch represented by 9.6×10^5 particles at collision energy. The relevant HL-LHC parameters considered are summarized in Table 1. Further studies including IP5 are foreseen.

Baseline Optics and Layout

The optics used for the whole machine is the HLLHCV1.0 collision optics, which includes the new Nb₃Sn triplet (140 T/m, 150 mm) with all the additional magnets needed to be compatible with $\beta^* = 0.15 \text{ m}$ and implementing the ATS scheme [6].

Crab Cavities

The HLLHCV1.0 optics include the installation of three CCs per IP, per side and per beam (n_{cc}). To simplify the opening and closing of the crab bump, the groups of $n_{\text{cc}} = 3$

Table 1: Relevant HL-LHC Nom. Parameters (25 ns)

Parameter	Symbol	Value
Beam energy at collision	E [TeV]	7
Particles per bunch	N	2.2×10^{11}
Bunches per beam	n_b	2748
Crossing angle (IP1 & IP5)	θ [μrad]	590
Minimum β^*	β^* [m]	0.15
Norm. transverse emittance	ϵ_n [μm]	2.50
RMS energy spread	σ_s [0.0001]	1.13
RMS bunch length	σ_l [cm]	7.55
CC RF frequency	f_{cc} [MHz]	400.79

CCs were installed next to each other at the same location. The parameters of the simulated CCs are summarized in Table 2. Further simulations using the current baseline optics HLLHCV1.1 [7] with $n_{cc} = 4$ is foreseen. The phase advance between the CCs and the IP is optimized to be $\Delta\phi = \frac{\pi}{2}$, and the voltage of the CCs is the one required to open the crab bump and produce an effective head-on collision [8], given by

$$V_{cc} = \frac{c \cdot E \cdot \tan(\varphi)}{q \cdot \omega_{cc} \cdot \sqrt{\beta^* \beta_{cc}} \cdot \sin(\Delta\phi) \cdot n_{cc}},$$

where ω_{cc} is the angular frequency of the CCs in [$\text{rad} \cdot \text{s}^{-1}$], β_{cc} is the value of the beta function at the location of the CC in [m], c is the speed of light and q the proton charge. Since the crossing angle in IP1 is in the vertical plane, the kick provided by the simulated CCs is also in the vertical plane.

Table 2: CC Parameters Used in the Simulation for IP1

Side	n_{cc}	s [m]	Voltage [MV]	β_{cc} [m]
Right	3	-147	3.19	4395
Left	3	149	3.23	4281

Collimation and Aperture

The collimation system [9, 10] is installed to safely dispose of unavoidable beam losses, but it also represents a passive protection for the machine during the dumping time (3 LHC turns = 266 μs) in case of a fast failure. The collimation system was included in the tracking simulations [11] in order to assess the limit in which the machine can cope with CC failures. The settings used in the simulations are summarized in Table 3.

The losses in the aperture are computed from the results of the tracking simulations of the full particle distribution, using a detailed aperture model of the full LHC ring. The spatial resolution of the model is 10 cm over the total length of 27 km [12].

Beam Distributions

For the transverse phase space, a 2D Gaussian distribution was generated for each plane. For the longitudinal plane, the

Table 3: Nominal Settings in Terms of σ ($\epsilon_n = 3.75 \mu\text{m}$)

Collimator	Opening [σ]
Primary IR7	6
Secondary IR7	7
Absorber IR7	10
Primary IR3	12
Secondary IR3	15.6
Absorber IR3	17.6
Secondary IR6	7.5
Dump protection IR6	8
Tertiary IR2/8	12
Tertiary IR1/5	8.3

2D Gaussian distribution was truncated in order to match the RF bucket (Fig. 1). The parameters of the gaussian distributions are given in Table 1. The same initial distribution was used for all the simulations.

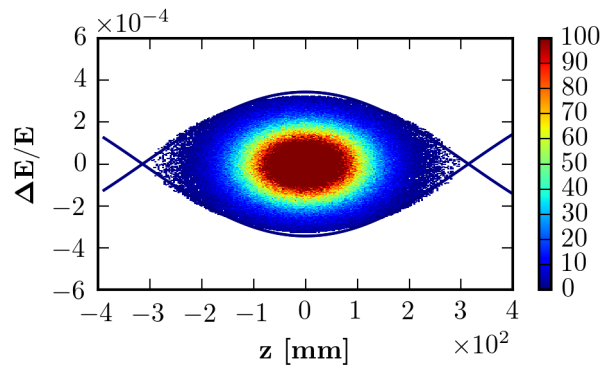


Figure 1: Initial distribution in the longitudinal plane. Arbitrary density units were used.

Simulated Cases

Five scenarios are considered:

- **No failure:** the particles are tracked for 51 turns in normal conditions.
- **Voltage failure of 3 CCs:** the voltage drops exponentially towards 0 V following $V(t) = V_0 \cdot e^{-t}$, where t is the turn number after onset of failure. The phase remains constant with a value of 0° .
- **Phase failure of 1, 2 & 3 CCs:** the phase jumps from 0° to 90° in one turn, while the voltage remains constant.

The failures are applied only to the group of CCs situated downstream, leaving the CCs upstream working normally. The particles are initially tracked for 10 turns. The failure takes place in the 11th turn, and the particles are tracked for 40 additional turns. Nevertheless, since the beam dumping time is of 3 turns, the losses after 3 turns are also considered.

FIRST RESULTS FROM DETAILED SIMULATIONS

Full simulations based on SIXTRACK with the newly implemented general dynamic kick module have started recently. We discuss here our first observations, which extend earlier studies [13–15].

A summary of the number of particles lost in the collimation system, in the aperture and the percentage of the total particles lost from the beam is shown in Table 4.

Table 4: Particle Losses Out of 9.6×10^5 Tracked Particles After 3 Turns After the Fault, and After 40 Turns After the Fault (Between Parenthesis).

Failure	Coll.	Aperture	[%]
None	102	0	0.01
Volt. (3/3 CCs)	689	0 (0)	0.07 (0.3)
Ph. (1/3 CC)	501	0 (0)	0.05 (0.2)
Ph. (2/3 CCs)	44118	4 (5)	4 (8)
Ph. (3/3 CCs)	311596	166 (186)	32 (39)

A simultaneous voltage failure of all CCs on one side results in a loss of 0.07% of the particles tracked.

Phase jumps of 90° in a single turn were considered in our simulations as worst case scenarios. They would result in a significant transverse kick of the densely populated bunch center (see Fig. 2). Studies are still ongoing in order to assess the real phase and voltage decay time of the CCs.

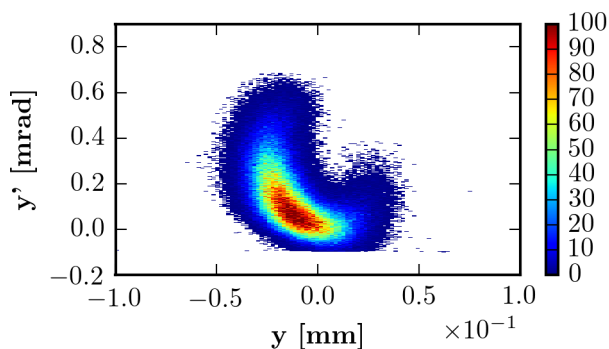


Figure 2: Transverse beam distribution in the crossing plane at IP1, after a phase trip of the 3 CCs downstream (after 1 turn). Arbitrary density units were used.

For a single CC, we observe a loss of 0.05% of the tracked particles, which is in good agreement with earlier studies [13–15]. For a phase jump of 2 CCs this increases to 4% and for 3 CCs to 32%. For this last case, we can see from Fig. 3 (top) that significant losses would start in the 11th turn, which corresponds to the turn of the phase failure. We can also see from Table 4 that almost all the losses occur within the first 3 turns. We see from Fig. 3 (bottom) that the primary IR7 collimators are the main aperture bottleneck which intercepts most losses, and only a small fraction hits the tertiary collimators.

This worst case scenario is considered to be unlikely, as the CC related hardware and control system can be designed

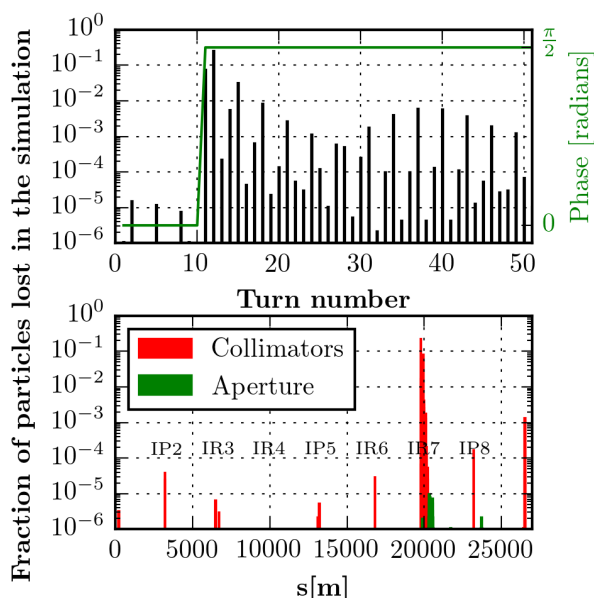


Figure 3: Losses around the ring for the simultaneous phase failure of 3 CCs (9.6×10^5 tracked particles) for 51 turns.

such that a simultaneous failure of these three independent modules is extremely unlikely. Mitigation techniques are also foreseen, in which the Multi-Cavity Feedback controller will adjust the field in the other cavities on both sides of the IP if the field starts changing in one of the CCs. This way the orbit distortions will remain local [4, Chapter 4]. Simulations indicate that if this technique is applied, the losses are reduced by 95%.

The losses are much less critical for the failure of a single CC, and could be mitigated by the introduction of devices such as hollow electron lenses [16].

SUMMARY AND OUTLOOK

We describe the simulation of CC failures using the new DYNK module within SIXTRACK. We also discuss first results for worst case voltage and phase failures, and observe that these could result in rather fast losses. The studies described here will be continued in close collaboration with the hardware side and in preparation of CC tests in the SPS, to make sure that any dangerous failure scenarios can be avoided to allow for a safe integration of CCs in LHC operation.

ACKNOWLEDGMENTS

The author would like to thank R. Bruce, M. Fiassaris and A. Rossi for their help and collaboration with the collimation files, M. Giovannozzi for the useful discussions about the aperture and A. Avilés for the computing suggestions.

REFERENCES

- [1] F. Schmidt. Single particle tracking code treating transverse motion with synchrotron oscillations in a symplectic manner. *CERN/SL/9456 (AP)*, 2012.

- [2] K. Sjobak et al. General functionality for turn-dependent element properties in SixTrack. In *these proceedings, MOPJE069, IPAC'15, Richmond, VA, USA, 2015.*
- [3] S. Fartoukh. Achromatic telescopic squeezing scheme and application to the LHC and its luminosity upgrade. *Phys. Rev. ST Accel. Beams*, 16:111002, Nov 2013.
- [4] *HL-LHC Preliminary Design Report*, volume V07. CERN, 2015.
- [5] R. Schmidt et al. Machine protection challenges for HL-LHC. In *Proceedings of IPAC'14, TUPRO016, Dresden, Germany, 2014.*
- [6] R.D. Maria et al. HLLHCv1.0: HL-LHC layout and optics models for 150 mm Nb3Sn triplets and local crab-cavities. In *Proceedings of IPAC'13, TUPFI014, Shanghai, China, 2013.*
- [7] R.D. Maria et al. HLLHCv1.1 optics version for the HLLHC upgrade. In *these proceedings, TUPTY037, IPAC'15, Richmond, VA, USA, 2015.*
- [8] Y-P. Sun et al. Beam dynamics aspects of crab cavities in the CERN large hadron collider. *Phys. Rev. ST Accel. Beams*, 12:101002, Oct 2009.
- [9] R.W. Assmann. Collimators and beam absorbers for cleaning and machine protection. In *Proceedings of the LHC Project Workshop - Chamonix XIV, Chamonix, France , 261, 2005.*
- [10] R.W. Assmann. The final collimation system for the LHC. In *Proc. of the European Particle Accelerator Conference, Edinburgh, Scotland , 986, 2006.*
- [11] G. Robert-Demolaize et al. A new version of sixtrack with collimation and aperture interface. In *Proceedings CERN-AB-2005-033, PAC-2005-FPAT081, 2005.*
- [12] S. Redaelli et al. LHC aperture and commissioning of the collimation system. In *Workshop Chamonix XIV, 2005.*
- [13] T. Baer et al. LHC machine protection against very fast crab cavity failures. In *Proceedings of IPAC'11, TUPZ009, San Sebastián, Spain, 2011.*
- [14] F. Bouly et al. Preliminary study of constraints, risks and failure scenarios for the High-Luminosity insertions at HL-LHC. In *Proceedings of IPAC'14, TUPRO016, Dresden, Germany, 2014.*
- [15] B. Yee-Rendon et al. Simulations of fast crab cavity failures in the high luminosity Large Hadron Collider. *Phys. Rev. ST Accel. Beams*, 17:051001, May 2014.
- [16] G. Stancari et al. Electron lenses for the Large Hadron Collider. In *Proceedings of IPAC'14, TUOBA01, Dresden, Germany, 2014.*